

Contents List available at JACS Directory

Journal of Advanced Chemical Sciences

journal homepage: www.jacsdirectory.com/jacs



Facile Synthesis and Characterization of ZnO/CuO Nanocomposite for Humidity Sensor Application

CH. Ashok, K. Venkateswara Rao*, CH. Shilpa Chakra

Centre for Nano Science and Technology, Institute of Science and Technology, Jawaharlal Nehru Technological University Hyderabad, Kukatpally Hyderabad, Telangana – 500 085, India.

ARTICLE DETAILS

Article history:
Received 02 November 2015
Accepted 30 December 2015
Available online 24 February 2016

Keywords: ZnO/CuO Ionic liquid Sensor

ABSTRACT

ZnO/CuO nanocomposite was synthesized by microwave-assisted technique using ionic liquid. The nanocomposite was studied by X-ray diffractometer (XRD), particle size analyser (PSA), scanning electron microscope (SEM), Fourier transform infrared spectrometer (FTIR) and thermo gravimetric and differential thermal analyser (TGDTA). The ZnO/CuO nanocomposite was confirmed by XRD with JCPDS card numbers along with average crystallite size in nano meter range. Average particle size was obtained as 28 nm and 34 nm for different temperatures. SEM images inferred that the nanocomposite shown high porous nature. The Zn-O and Cu-O stretching bands were observed in FTIR. The weight losses of the sample and phase transformation details were obtained by TGDTA. The humidity sensing property of the nanocomposite increased along with increasing of annealing temperature.

1. Introduction

Generally the researchers are showing extensive interest towards semiconductor nanomaterials because of their potential use in wide range of applications like catalysis [1], optoelectronics [2], hydrogen storage [3], information storage [4] and sensors [5]. ZnO/CuO nanocomposite material is having high stability, chemical reactivity, photocatalytic activity, low cost and environmental friendly [6]. ZnO is n-type semiconductor material with wide band gap (3.37 eV) and CuO is p-type semiconductor material with narrow band gap (1.7 eV). The hetero junctions of n-type ZnO and p-type CuO nanocomposite improved the electron-hole separation [7]. In general, combination of narrow band gap semiconductors with wide band gap semiconductors will increase their sensing property [8, 9]. These nanocomposites are used in several applications such as solar cells [10], gas sensors [11], biosensors [12], humidity sensors [13]. These obtained nanocomposite material showed dissimilar morphologies: nano-rings, nano-combs, nano-belts, nano-tubes, nano-rods and nano-sheets [14]. Many synthesis techniques are offered to prepare nanocomposite material. The techniques are plasma-enhanced chemical vapour deposition [15], hydrothermal [16], sol-gel [17], precipitation [18], electrochemical [19] and microwave-assisted method [20]. In this present paper, the ZnO/CuO nanocomposite was successfully prepared by room temperature ionic liquid with microwave-assisted synthesis technique. Room temperature ionic liquids were used in the reaction for the sake of different nanostructures formation. These room temperature ionic liquids also having the unique properties like wide liquid temperature range, high thermal stability and exceptional microwave absorbing ability. Microwave-assisted synthesis technique is used for the homogeneous heating and reaction controlling. The present work deals with the preparation of ZnO/CuO nanocomposite and its humidity sensor application.

2. Experimental Methods

Zinc acetate, copper acetate, 1-butyl-3-methyl imidazolium tetrafluoro borate ([bmim]BF4), and sodium hydroxide (NaOH) were used as the precursor materials for $\rm ZnO/CuO$ nanocomposite preparation. $\rm ZnO$ and $\rm CuO$ nanomaterials was prepared individually and mixed using milling

method. Zinc acetate (0.1 M), NaOH (0.1 M) solutions were prepared in two separate beakers and added by continuous stirring. After 30 minutes of stirring 0.8 mL of [bmim]BF₄ ionic liquid was added. This solution was kept in microwave irradiation for 5 minutes. Finally the precipitate was formed; this precipitate was washed several times with water, ethanol and further dried for 90 minutes at 60 °C. The same process was followed to prepare CuO nanomaterials. ZnO/CuO nanocomposite was prepared by manual grinding of a mixture containing ZnO and CuO by using mortar and pestle for 60 minutes. The composition of ZnO and CuO was 1:1 wt%.

2.1 Characterization Techniques

The crystal structure and average crystallite size was measured by BRUKER D8 X-ray diffractometer using CuK α_1 -radiation (λ = 0.154 nm). HORIBA SZ-100 Particle Size Analyser used for average particle size measurement. The surface morphology of the sample was obtained from S 3400 N scanning electron microscope. Metal – oxygen stretching vibrations of the sample was examined by BRUKER Fourier Transform Infrared Spectrometer. The thermal properties of the sample attained by EXTRAR 6000 Thermo Gravimetric and Differential Thermal Analyser

3. Result and Discussion

3.1 X-Ray Analysis

XRD pattern of ZnO/CuO nanocomposite is shown in Fig. 1. The diffraction peaks were well defined and good agreement with JCPDS card numbers 36-1451 and 89-5899 for ZnO (hexagonal) and CuO (monoclinic) respectively. The sharp peaks represents that the obtained nanocomposite is having high crystallinity nature. The Table 1 showed the XRD peak position, d-spacing and miller indices.

The below data concludes that the obtained the ZnO/CuO nanocomposite has been formed. The d-spacing values of ZnO/CuO nanocomposite from JCPDS card numbers is almost equal to d-spacing values measured from Bragg's law. The miller indices also shown in the Table 1, the bar inferred that the negative direction of the miler indices.

*Corresponding Author

Email Address: kalagadda2003@gmail.com (K. Venkateswara Rao)

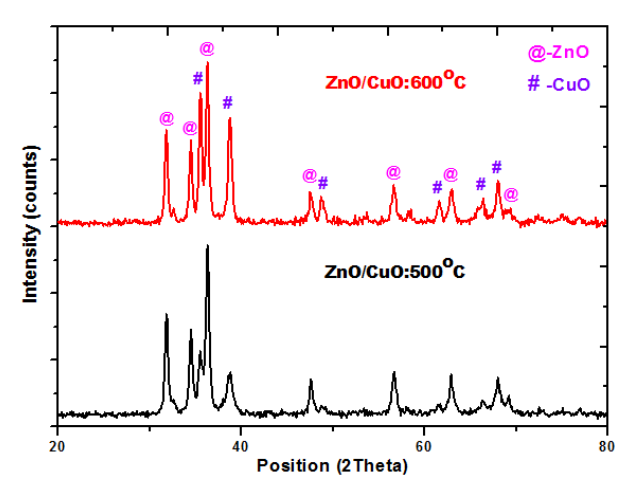


Fig. 1 XRD pattern of ZnO/CuO nanocomposite synthesised at different temperature

Table 1 XRD position, d-spacing and miller indices

S.No.	Position	Comp	ound	d-spacing	d-spacing	Miller
	(degree)	Zn0	Cu0	(from	(By Bragg's	Indices
				JCPDS)	Law)	
1.	31.8	$\sqrt{}$		2.8143	2.8106	(100)
2.	34.4	$\sqrt{}$		2.6033	2.6039	(0 0 2)
3.	35.5		$\sqrt{}$	2.5227	2.5257	$(\overline{1}11)$
4.	36.2	$\sqrt{}$		2.4759	2.4785	(101)
5.	38.7		$\sqrt{}$	2.3214	2.3239	$(1\ 1\ 1)$
6.	47.6	$\sqrt{}$		1.9111	1.9081	(102)
7.	48.7		$\sqrt{}$	1.8681	1.8675	$(\bar{2}\ 0\ 2)$
8.	56.7		$\sqrt{}$	1.6199	1.6215	(0 2 1)
9.	61.6		$\sqrt{}$	1.5052	1.5038	$(\overline{1}13)$
10.	62.9	$\sqrt{}$		1.4771	1.4758	(103)
11.	66.3	$\sqrt{}$		1.4071	1.4081	(200)
12.	68.0		$\sqrt{}$	1.3747	1.3770	(2 2 0)
13.	69.2	$\sqrt{}$		1.3582	1.3560	(2 0 1)

The average crystallite size was measured by Debye-Scherrer's formula,

$D = K\lambda/\beta \cos\theta$

Where K-Debye-Scherrer's constant, λ -Wavelength of the radiation (CuK α_1 =0.154 nm), β -Full Width Half Maximum (FWHM) and θ -Bragg's angle.

The average crystallite size was measured as 22 nm and 28 nm for different annealing temperatures. This inferred that when annealing temperature increases the average crystallite was increased because of the internal bond breaking [21].

3.2 Particle Size Analyser

The particle size distribution in the particle size analyser was shown in Fig. 2. The ZnO/CuO nanocomposite (0.001 mg) was dispersed in 5 mL of ethanol solution and to measure the average particle size.

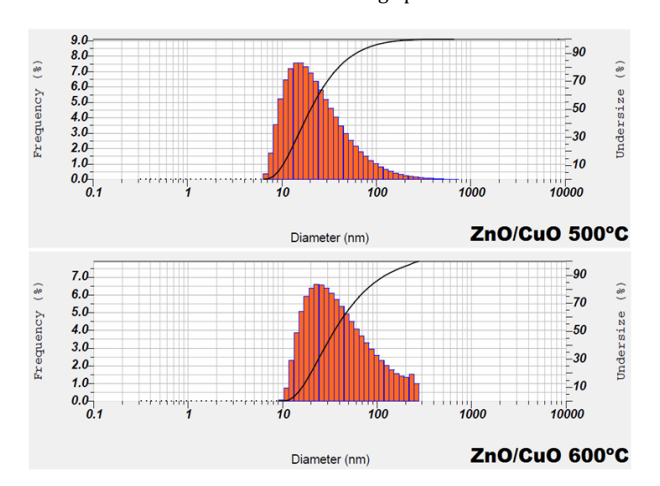


Fig. 2 Particle size distribution at a) 500 °C and b) 600 °C

The histograms were recorded from particle size analyser due to the Brownian motion of the dispersed solution. The average particle size was taken as the mean value of the histogram. The average particle size was obtained as 34 nm and 46 nm for different annealing temperatures. The average crystallite size from XRD was less than the average particle size from particle size analyser. This data was matched with the Ashok et al [22].

3.3 Scanning Electron Microscope

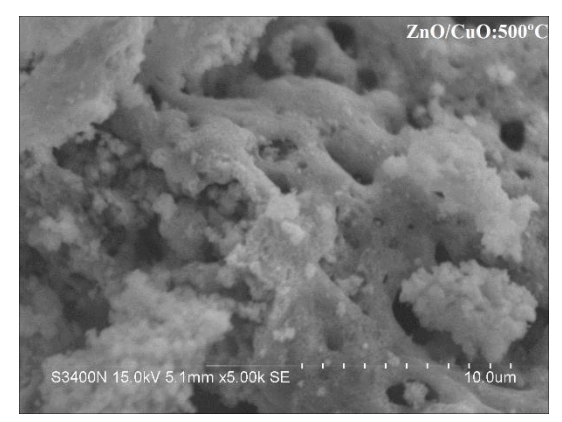
The SEM images of ZnO/CuO nanocomposite at different annealing temperature were shown in Fig. 3a and b.

The porosity was measured by the following equation

$$P(\%) = \frac{(\rho_{\text{th}} - \rho_{\text{a}})}{\rho_{\text{th}}} \times 100$$

Where ρ_{th} -theoretical density and ρ_a -actual density

The porosity of the ZnO/CuO nanocomposite at 500 °C annealing temperature was 3.764% and at 600 °C it was 4.258 % (The theoretical density of ZnO/CuO composite is 4.7476 g/cc). This showed that when the annealing temperature increased the porosity of the nanocomposite was also increased because of the agglomeration (when temperature increases agglomerations are found. More the agglomeration lesser the surface to volume ratio and more the porosity of the material) [23].



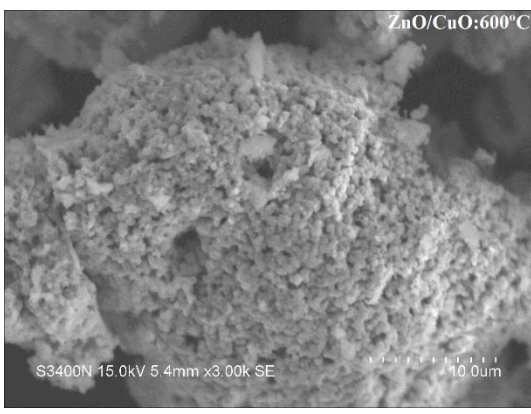


Fig. 3 SEM image of ZnO/CuO Nanocomposite at a) 500 °C and b) 600 °C

The SEM images also visualised that the ZnO/CuO nanocomposite at $600\,^{\circ}\text{C}$ annealing temperature was highly porous compared with ZnO/CuO nanocomposite at $500\,^{\circ}\text{C}$ annealing temperature. This was occurred due to temperature increase. When temperature increased the agglomeration takes place, depending on the agglomeration the particle size increased. The particle size increment causes the increasing of porosity. This data was compared with Venkateswara Rao et al shows the equality of the SEM images [24].

3. 4 Fourier Transform Infrared Spectroscopy

The ZnO/CuO nanocomposite was admixed with KBr powder and to make a pellet using high pressures. These pellets were characterised with the help of FTIR spectrometer. The Fourier transform infrared spectrum of ZnO/CuO nanocomposite was shown in Fig. 4a and b. The strong peaks around $1600~\rm cm^{-1}$ and $3460~\rm cm^{-1}$ indicates that the stretching band of water molecules as well as hydroxyl groups which is on the surface of ZnO/CuO nanocomposite.

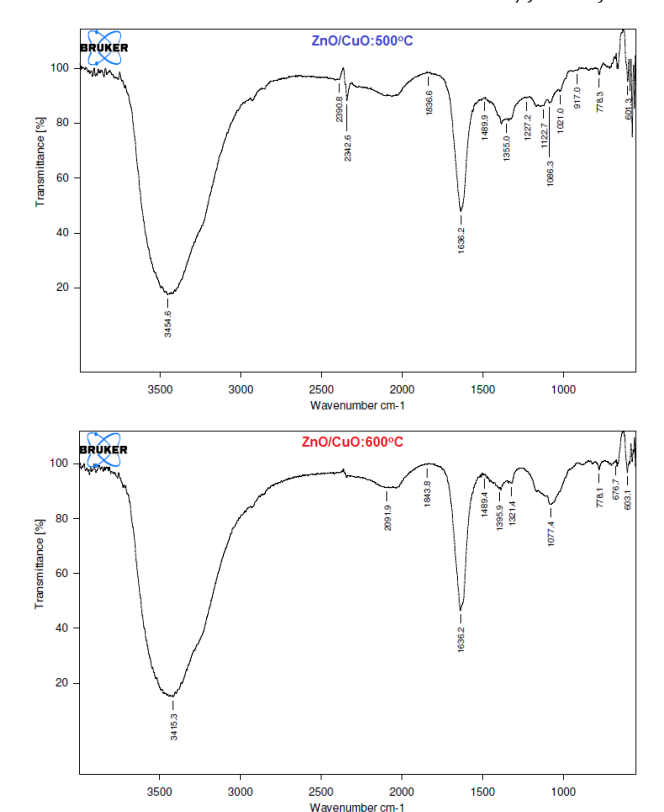


Fig. 4 FTIR spectrum of ZnO/CuO nanocomposite at a) 500 °C and b) 600 °C

The weak vibration of absorbed CO_2 was conformed in between 1836 cm $^{-1}$ to 2390 cm $^{-1}$. Peaks around 1100 cm $^{-1}$ to 1500 cm $^{-1}$ concluded the presence of C-H vibration of stretching band. Zn-O stretching band was observed within the range of 700 cm $^{-1}$ to below 1100 cm $^{-1}$. The Cu-O stretching band was obtained around 600 cm $^{-1}$. FTIR stretching bands were reported by Fung et al stated about CuO stretching band [25].

4.5 Thermo Gravimetric and Differential Thermal Analyser

Thermo gravimetric and differential thermal analyser is used to measure the thermal properties of the nanocomposites. The weight loss and differential thermal analysis was studied with the function of temperature varying from room temperature to 800 °C. In both cases of 500 °C and 600 °C annealing temperatures the weight losses were obtained as 1.7% and 1.4% respectively (Fig. 5). This weight decrement observed due to the increasing of annealing temperature.

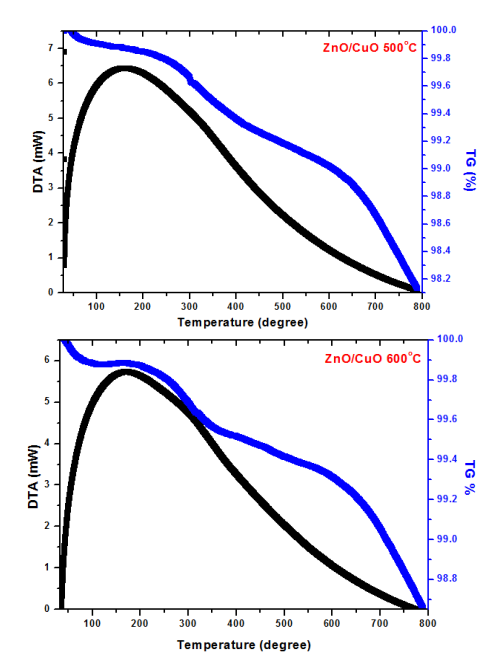


Fig. 5 TG/DTA Graph for ZnO/CuO Nanocomposite at a) 500 $^{\circ}\text{C}$ and b) 600 $^{\circ}\text{C}$

The weight loss occurred from room temperature to around 100 °C is due to the evaporation of water molecules. From 100 °C to 350 °C the weight loss was obtained due to the evaporation of inorganic materials. From 350 °C to 800 °C the weight loss gained from the evaporation and combustion of organic materials in the sample. This was explained by Chang et al [26].

4.6 Humidity Sensor Application

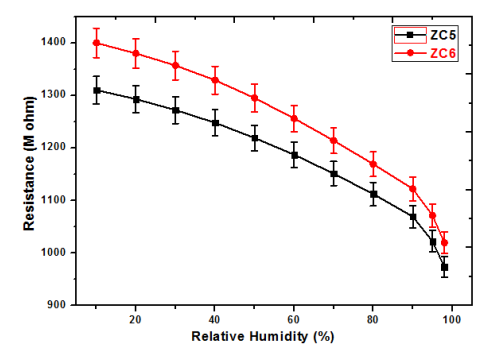
The sensitivity (S) of a humidity sensor has been defined as a change in resistance (ΔR) of a sensing element per unit change in relative humidity (ΔRH).

 $S = \Delta R /_{\Delta RH}$

The pellets were made by ZnO/CuO nanocomposite. This pellet was placed in between two Cu-electrodes, and the digital multimeter was connected to the edges of the electrodes. This complete set-up was kept in controlled humidity chamber. The resistance measurement of ZnO/CuO nanocomposite as a function of relative humidity (%) was shown in Fig. 6. The resistance studies were measured from RH 10% to RH 98% was shown in Table 2. The resistance value of ZnO/CuO nanocomposite decreased as RH% increase in both cases.

Table 2 Resistance of ZnO/CuO Nanocomposite

RH (%)	Resistance (MΩ)	Resistance (MΩ)
	ZnO/CuO at 500 °C	ZnO/CuO at 600 °C
10	1310	1400
20	1293	1380
30	1272	1357
40	1248	1329
50	1219	1295
60	1187	1256
70	1151	1214
80	1112	1169
90	1069	1123
95	1022	1071
98	973	1019



 $\textbf{Fig. 6} \ \textbf{Resistance} \ \textbf{in the function of Relative Humidity}$

The decrements of resistance obtained due to the increase of humidity (Presence of water vapour). The resistance value decreased from $1310\,M\Omega$ to $973\,M\Omega$ and $1400\,M\Omega$ to $1019\,M\Omega$ for RH 10% to 98% of both annealing temperatures. Srivastava et al reported nanocomposite humidity sensing property, the sensitivity compared by ZnO/CuO nanocomposite and these composites were showing almost similar results [27].

The sensitivity of ZnO/CuO nanocomposite was measured by the above mentioned formula. The sensitivity is increased along with increasing of RH% shown in Table 3. The graphical representation of sensitivity increment was shown in Fig. 7. The porosity of the ZnO/CuO nanocomposite played an important role in the increasing of sensitivity. The sensitivity values were increased at ZnO/CuO nanocomposite at annealing temperature 600 $^{\circ}\text{C}$ when compared with 500 $^{\circ}\text{C}$. This was happened due to the increasing of porosity of the nanocomposite as visualised in SEM.

Table 3 Sensitivity of ZnO/CuO Nanocomposite

RH (%) Sensitivity (S) ZnO/CuO at 500 °C Sensitivity (S) ZnO/CuO at 600 °C 15 1.7 2.0 25 2.1 2.3 35 2.4 2.8 45 2.9 3.4 55 3.2 3.9 65 3.6 4.2 75 3.9 4.5 85 4.3 4.7 95 4.6 5.1 98 4.9 5.3		<u> </u>		
15 1.7 2.0 25 2.1 2.3 35 2.4 2.8 45 2.9 3.4 55 3.2 3.9 65 3.6 4.2 75 3.9 4.5 85 4.3 4.7 95 4.6 5.1	RH (%)	Sensitivity (S)	Sensitivity (S)	
25 2.1 2.3 35 2.4 2.8 45 2.9 3.4 55 3.2 3.9 65 3.6 4.2 75 3.9 4.5 85 4.3 4.7 95 4.6 5.1		ZnO/CuO at 500 °C	ZnO/CuO at 600 °C	
35 2.4 2.8 45 2.9 3.4 55 3.2 3.9 65 3.6 4.2 75 3.9 4.5 85 4.3 4.7 95 4.6 5.1	15	1.7	2.0	
45 2.9 3.4 55 3.2 3.9 65 3.6 4.2 75 3.9 4.5 85 4.3 4.7 95 4.6 5.1	25	2.1	2.3	
55 3.2 3.9 65 3.6 4.2 75 3.9 4.5 85 4.3 4.7 95 4.6 5.1	35	2.4	2.8	
65 3.6 4.2 75 3.9 4.5 85 4.3 4.7 95 4.6 5.1	45	2.9	3.4	
75 3.9 4.5 85 4.3 4.7 95 4.6 5.1	55	3.2	3.9	
85 4.3 4.7 95 4.6 5.1	65	3.6	4.2	
95 4.6 5.1	75	3.9	4.5	
	85	4.3	4.7	
98 4.9 5.3	95	4.6	5.1	
	98	4.9	5.3	

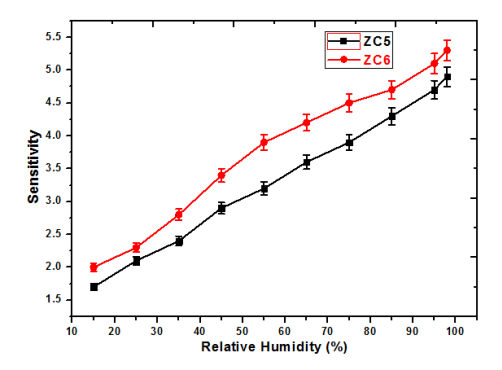


Fig. 7 Sensitivity in the function of Relative Humidity

In this sensing material the cations were actively participated in the adsorption due to the high charge density. These ions were readily associated with the hydroxyl group of adsorbed water, due to this reason the electrical conduction was increased, means the resistance was decreased. The response time and recovery time of the sensing elements were noticed as 172 s and 495 s for 500 °C annealing nanocomposite, whereas at 600 °C it has 158 sec and 426 sec respectively. Pandey et al mentioned about response and recovery times, these ZnO/CuO nanocomposite nearly reached to reported value [28].

4. Conclusion

ZnO/CuO nanocomposite was successfully prepared by microwaveassisted synthesis using room temperature ionic liquids. The crystal structure and average crystallite was measured by X-ray diffractometer, the peaks conformed that the obtained nanocomposite was ZnOhexagonal and CuO-monoclinic structures, and there was no external phases involved in the nanocomposite. The average particle size of the nanocomposite was obtained from particle size analyser. The average crystallite size from XRD was less than to the average particle size from particle size analyser. SEM images of nanocomposite showed porous nature. FTIR supported to the XRD with respect to no phase transformation. When annealing temperature increased the weight loss decreased; it was confirmed by TG/DTA. The sensitivity of the ZnO/CuO nanocomposite increased with annealing temperature. The response time and recovery time also decreased along with increasing of annealing temperature. Among all the above data, the ZnO/CuO nanocomposite at 600 °C annealing temperature was showed better sensing properties compared with 500 °C.

Acknowledgement

The authors would like to thank for the financial support provided by University Grants Commission, New Delhi, Government of India for carrying out this research work.

References

- M. Sabbaghan, A. Ghalaei, Catalyst application of ZnO nanostructures in solvent free synthesis of polysubstituted pyrroles, J. Mol. Liq. 193 (2014) 116-122.
- [2] A.B. Djurisic, A.M.C. Ng, X.Y. Chen, ZnO nanostructures for optoelectronics: Material properties and device applications, Prog. Quan. Elect. 34 (2010) 191-250
- [3] M. Ahmad, Rafi-ud-Din, C. Pan, J. Zhu, Investigation of hydrogen storage capabilities of ZnO-based nanostructures, J. Phys. Chem. C. 114 (2010) 2560– 2565
- [4] X. Xia, Y. Zhang, D. Chao, C. Guan, Y. Zhang, L. Li, X. Ge, I. Mínguez Bacho, J. Tu, H. Jin Fan, Solution synthesis of metal oxides for electrochemical energy storage applications, Nanoscale 6 (2014) 5008-5048.
- [5] R. Srivastava, B.C. Yadav, Nanostructured ZnO, ZnO-TiO₂ and ZnO-Nb₂O₅ as solid state humidity sensor, Adv. Mat. Lett. 3 (2012) 197-203.
- [6] W. Ang, X. Li, S. Li, L. Yan-Jun, L. Wei-Wei, CuO nanoparticle modified ZnO nanorods with improved photocatalytic activity, Chin. Phys. Lett. 30 (2013) 046202.
- [7] Z. Chen, S. Li, Y. Tian, S. Wu, W. Zhang, Synthesis of magnesium oxide doped zno nanostructures using electrochemical deposition, Int. J. Electrochem. Sci. 7 (2012) 10620-10626.
- [8] R. M. Állaf, L. J. Hope-Weeks, Synthesis of ZnO-CuO nanocomposite aerogels by the sol-gel route, J. Nanomater. 2014 (2014) 491817.
- [9] Y. Caglar, D. Duygu Oral, M. Caglar, S. Ilican, M. Allan Thomas, K. Wu, Z. Sun, J. Cui, Synthesis and characterization of (CuO)_x(ZnO)_{1-x} composite thin films with tunable optical and electrical properties, Thin Solid Films 520 (2012) 6642–6647.
- [10] E.O. Omayio, P.M. Karimi, W.K. Njoroge, F.K. Mugwanga, Current-voltage characteristics of p-CuO/n-ZnO:Sn Solar cell, Int. J. Thin Film Sci. Technol. 2 (2013) 25-28.
- [11] Y. Zhu, C. Haur Sow, T. Yu, Q. Zhao, P. Li, Z. Shen, D. Yu, J. Thiam-Leong Thong, Co-synthesis of ZnO-CuO nanostructures by directly heating brass in air, Adv. Funct. Mater. 16 (2006) 2415–2422.
- [12] T. Soejima, K. Takada, S. Ito, Alkaline vapor oxidation synthesis and electrocatalytic activity toward glucose oxidation of CuO/ZnO composite nanoarrays, Appl. Surf. Sci. 277 (2013) 192–200.
- [13] A. Zainelabdin, G. Amin, S. Zaman, O. Nur, J. Lu, L. Hultman, M. Willander, CuO/ZnO nanocorals synthesis via hydrothermal technique: growth mechanism and their application as humidity sensor, J. Mater. Chem. 22 (2012) 11583–11590.
- [14] Q. Wei, G. Meng, X. An, Y. Hao, L. Zang, Temperature controlled growth of ZnO nanostructure: branched nanobelts and wide nanosheets, Nanotechnol. 16 (2005) 2561-2566.
- [15] Q. Simon, D. Barreca, A. Gasparotto, C. Maccato, E. Tondello, C. Sada, et al., CuO/ZnO nanocomposite gas sensors developed by a plasma-assisted route, Chem. Phys. Chem. 13 (2012) 2342–2348.
- [16] T. Chang, Z. Li, G. Yun, Y. Jia, H. Yang, Enhanced photocatalytic activity of ZnO/CuO nanocomposites synthesized by hydrothermal method, Nano-Micro Lett. 5 (2013) 163-168.
- [17] M.H. Habibi, B. Karimi, M. Zendehdel, M. Habibi, Fabrication, characterization of two nano-composite CuO-ZnO working electrodes for dye-sensitized solar cell, Spectrochim. Acta. A. Mol. Biomol. Spectrosc. 116 (2013) 374-380.
- [18] B. Li, Y. Wang, Facile synthesis and photocatalytic activity of ZnO-CuO nanocomposite, Superlattice Microst. 47 (2010) 615-623.
- [19] G. Chaitanya Lakshmi, S. Ananda, R. Somashekar, C. Ranganathaiah, Synthesis of ZnO/MgO nanocomposites by electrochemical method for photocatalytic degradation kinetics of Eosin yellow dye, Int. J. NanoSci. Nanotechnol. 3 (2012) 47-63
- [20] R.N. Gedye, F.E. Smith, K.C. Westaway, The rapid synthesis of organic compounds in microwave ovens, Can. J. Chem. 66 (1988) 17-26.
- [21] F. Jamali Sheini, J. Singh, O.N. Srivasatva, D.S. Joag, M.A. More, Electrochemical synthesis of Cu/ZnO nanocomposite films and their efficient field emission behaviour, Appl. Surf. Sci. 256 (2010) 2110-2114.
- [22] CH. Ashok, K. Venkateswara Rao, CH. Shilpa Chakra, Structural properties of CdS nano particles prepared in the presence of organic solvent, Adv. Appl. Sci. Res. 5 (2014) 99-105.
- [23] B.C. Yadav, R. Srivastava, C.D. Dwivedi, Synthesis and characterization of ZnO nanorods by the hydroxide route and their application as humidity sensors, Syn. React. Inorg. Met. 37 (2007) 417-423.
- [24] K. Venkateswara Rao, C.S. Sunandana, Structure and microstructure of combustion synthesized MgO nanoparticles and nanocrystalline MgO thin films synthesized by solution growth route, J. Mater. Sci. 43 (2008) 146-154.
- [25] Y. Fang, R. Wang, G. Jiang, Hejin, Y. Wang, X. Sun, S. Wang, T. Wang, CuO/TiO₂ nanocrystals grown on graphene as visible-light responsive photocatalytic hybrid materials, Bull. Mater. Sci. 35 (2012) 495-499.
- [26] C. Sung Lim, Synthesis and characterization of TiO₂-ZnO nanocomposite by a two-step chemical method, J. Ceramic. Proc. Res. 11 (2010) 631-635.
- [27] A.K. Srivastava, B.C. Yadav, Humidity sensing properties of TiO₂-Sb₂O₅ nanocomposite, Mater. Sci. Poland 28 (2010) 491-502.
- [28] N.K. Pandey, K. Tiwari, A. Roy, ZnO-TiO₂ nanocomposite: characterization and moisture sensing studies, Bull. Mater. Sci. 35 (2012) 347-352.